Kinetic and Mutational Studies of the Number of Interacting Divalent Cations Required by Bacterial and Human Methionine Aminopeptidases†

Xiaoyi V. Hu,‡ Xiaochun Chen,‡ Kee Chung Han,‡ Albert S. Mildvan,*,§ and Jun O. Liu*,‡,||

Departments of Pharmacology and Molecular Sciences and Biological Chemistry and Solomon H. Snyder Department of Neuroscience, The Johns Hopkins University School of Medicine, 725 North Wolfe Street, Baltimore, Maryland 21205

Received June 7, 2007; Revised Manuscript Received August 29, 2007

ABSTRACT: Methionine aminopeptidases (MetAP) are responsible for the proteolytic removal of the initiator methionine from nascent proteins. This processing permits multiple posttranslational modifications and protein turnover. We have cloned, expressed in *Escherichia coli*, and purified the recombinant human mitochondrial MetAP isoform (MetAP1D). The full-length enzyme and a truncated form lacking the mitochondrial targeting sequence (residues 1−55) have been characterized as metal-requiring proteases, with Co^{2+} being the best activator. At the optimal pH (8.0), the k_{cat} of MetAP1D of 0.39 min^{-1} is 280-fold lower, and the K_m of the substrate Met-Pro-*p*-nitroanilide (576 μM) is 3-fold greater, than the respective kinetic parameters obtained with MetAP from *E. coli*, although MetAP1D is 61% homologous to *E. coli* MetAP and their circular dichroic spectra are nearly identical. MetAP1D thus appears to be a less efficient enzyme than other known MetAPs in vitro. At saturating substrate concentrations, a plot of V_{max} versus free Co^{2+} shows sigmoidal metal activation of MetAP1D, both with and without an N-terminal His-tag, with a Hill coefficient (n) of 1.9 and a $K_{0.5}$ of 0.40 μM. Similarly, *E. coli* MetAP shows $n = 2.1$ and $K_{0.5} = 0.2$ μM. Hence, at least two Co^{2+} ions, which may act cooperatively, are needed to promote catalysis, providing kinetic evidence for the functioning of both Co^{2+} ions of the binuclear complex found in the X-ray structure of *E. coli* MetAP [Roderick, S. L. and Matthews, B. W. (1993) *Biochemistry 32*, 3907−3912] and resolving a disagreement in the literature. The X-ray structure of the human cytosolic MetAP1 showed three Co^{2+} ions at the active site, with the third Co^{2+} coordinated by the conserved residue His 212 [Addlagatta, A., Hu, X., Liu, J. O., and Matthews, B. W. (2005) *Biochemistry 44*, 14741−14749]. Consistent with the structure, kinetic studies of the human cytosolic MetAP1 yielded a Hill coefficient (n) of 2.9 and a $K_{0.5}$ of 0.26 μM for activation by Co^{2+}, as well as a k_{cat} of 25.5 min^{-1} and a K_m of 740 μM for the substrate Met-Pro-*p*-nitroanilide. The H212A mutation decreased n to 2.2, decreased k_{cat} 60-fold to 0.42 min^{-1}, and increased $K_{0.5}$ 6.5-fold to 1.8 μM. The H212K mutation further decreased n to 1.4, decreased k_{cat} 1800-fold to 0.014 min^{-1}, and increased $K_{0.5}$ 158-fold to 41 μM. Hence, at least three Co^{2+} ions are needed to promote optimal catalysis by human MetAP1. Both mutations of His212 abolished the binding and/or the cooperativity of the third Co^{2+} ion, as indicated by the decreases in n and the increases in $K_{0.5}$ of the remaining two Co^{2+} ions, but did not affect the K_m of the substrate. The more damaging effects of the H212K mutation on both the Hill coefficient for Co^{2+} binding and the catalysis suggest that Lys 212 might directly compete with Co^{2+} for the third metal-binding site. Together, these results suggest that human MetAP1 is distinct from other members of the MetAP superfamily in the number of metal ions employed and likely mechanism of catalysis.

Structural studies of metal-activated enzymes occasionally show two or more divalent cations sharing common ligands at the active site to form binuclear or higher complexes (*1*−*4*). In hydrolases, the shared ligands may include a nucleophile derived from water, such as hydroxide. While coordination by a second metal cation would facilitate the deprotonation of water to form hydroxide by the combined electrophilic effects of the two metals, the presence of the second metal would decrease the nucleophilicity of the metal-bound hydroxide by occupying one of its lone pairs of electrons (*2*, *5*). Three possible rationales have been proposed to explain the paradoxical existence of the second metal-binding site: (i) The second metal ion is not required for catalysis but is populating a second site because of the high metal ion concentrations used in the crystallization media. (ii) The second metal ion is required to form the hydroxide but dissociates from the shared hydroxide prior to nucleophilic attack. (iii) The attacking nucleophile is actually a doubly deprotonated oxide dianion shared by both metal cations (*2*, *5*). Average metal to oxygen distances are shorter

† This work was supported in part by NIH Grant CA078743 to J.O.L. and the Keck Center support to J.O.L. X.V.H. was supported by Predoctoral Fellowship W81XWH-04-1-0361 from the DoD Breast Cancer Research Program. X.C. was supported by Johns Hopkins School of Medicine, the Keck Foundation, and the Malaria Research Institute of Johns Hopkins Bloomberg School of Public Health.

* Corresponding authors: (J.O.L.) phone (410) 955-4619, fax (410) 955-4620, e-mail joliu@jhu.edu; (A.S.M.) phone (410) 955-2038, fax (410)-955-5759, e-mail mildvan@jhmi.edu.

‡ Department of Pharmacology and Molecular Sciences.

§ Department of Biological Chemistry.

|| Solomon H. Snyder Department of Neuroscience.

10.1021/bi701127x CCC: $37.00
Published on Web 10/11/2007

in oxides than in hydroxides of Zn^{2+}, Co^{2+}, and Mg^{2+} by 0.07, 0.14, and 0.14 Å respectively. Such small differences can be resolved crystallographically in small metal complexes (*5*) but only rarely in proteins, where the resolution is usually too low.

Methionine aminopeptidases (MetAP)[1] catalyze the important posttranslational hydrolytic removal of the initiator methionine from many proteins, which is required for their proper subcellular localization, function, and degradation (*6*). Their physiological significance is underscored by the lethal phenotypes of knockout mutants in *Escherichia coli* (*7*), *Salmonella typhimurium* (*8*), and *Saccharomyces cerevisiae* (*9*). Most prokaryotic organisms have only one MetAP gene, while eukaryotic organisms express at least two different isoforms of MetAP, types 1 and 2. MetAP2 contains an inserted domain of about 60 amino acids in comparison with MetAP1 (*10*). Human MetAP2 has been identified as the physiological target of the anti-angiogenic natural products fumagillin and ovalicin (*11*, *12*). Inhibition of MetAP2 has been found to activate the p53 pathway and to induce p21, the G_1 cyclin-dependent protein kinase inhibitor, leading to arrests in the endothelial cell cycle at the G_1/S transition (*13*, *14*). Recently, the use of isoform-selective inhibitors has also revealed the important function of human MetAP1 during the G_2/M transition of the cell division cycle (*15*).

A new isoform of MetAP, MetAP1D, was recently reported to be expressed in human cells and indicated to function in the mitochondria (*16*). MetAP1D is overexpressed in colon cancer cell lines and in colon tumors (*17*). Its downregulation by a small hairpin RNA in HCT-116 colon carcinoma cells reduces their anchorage-independent growth in soft agar, suggesting that MetAP1D may play an important function in oncogenesis (*17*).

Structural studies of MetAPs from *E. coli*, *Mycobacterium tuberculosis*, *Staphylococcus aureus* and *Pyrococcus furiosus* revealed two active-site divalent cations, typically Co^{2+}, which share the conserved ligands Asp108 and Glu 235 (*E. coli* numbering) and a water molecule, forming a binuclear complex (*18*−*21*). Unlike the prokaryotic MetAPs, human cytoplasmic MetAP1 holoenzyme contains, in addition to the two Co^{2+} ions shared by the conserved Asp240 and Glu367 ligands (human MetAP1 numbering), a third Co^{2+} that is coordinated by the conserved residue His212, forming a trinuclear complex (*22*). This observation further fueled the ongoing debate in the literature as to whether the MetAP reaction requires one, two, or possibly three divalent cations for full activity (*18*, *22*−*25*).

A convenient *functional* test of whether the additional metals are actually required for catalysis is based on our previous observation that binuclear (or higher) metal complexes of enzyme and substrate may form cooperatively, that is, the binding of the first metal cation to the enzyme−substrate complex raises the affinity of the active site for the second metal cation (*26*−*28*). Moreover, even in the absence of cooperativity, if no activity occurs until two or three metal-binding sites are populated, a plot of reaction velocity versus free metal ion concentration, at saturating substrate, can be fit by the Hill equation (*29*) to generate the Hill coefficient (n) for the catalytically functional binding of free metal. The Hill coefficient provides a lower limit to the number of essential metal ions in catalysis. Consistent with structural observations, such functional kinetic studies have previously detected multiple essential metal requirements for a reverse transcriptase ($n = 2$) (*26*), the 3′,5′ exonuclease of DNA polymerase I ($n = 2.4$) (*27*), and Ap_4A pyrophosphatase ($n = 3$) (*28*).

In this study, we have cloned, expressed in *E. coli*, and purified the recombinant full-length human mitochondrial MetAP1D and a truncated mutant (ΔTS-MetAP1D) lacking residues 1−55, the mitochondrial targeting sequence. Our kinetic characterizations demonstrate that MetAP1D belongs to the family of metal-activated proteases with Co^{2+} being the best activator.[2] The optimal pH and kinetic constants have been determined for MetAP1D. We have also carried out functional, kinetic studies of metal activation of MetAP1D along with methionine aminopeptidases from *E. coli* and human cytosol (MetAP1), which clarified the number of essential metal ions required by each enzyme. A preliminary abstract of this work has been published (*30*).

EXPERIMENTAL PROCEDURES

Cloning, Expression, and Purification. Human MetAP1D cDNA was cloned by RT-PCR with TRIZOL (Invitrogen) and SuperScript II reverse transcriptase from Invitrogen (Carlsbad, CA). The full-length open reading frame was subcloned into the pET28a vector (Novagen) by use of the following primers: forward, 5′-GCGGCTAGCAACATGGCGGCGCCCAGTGG, and reverse, 5′-GCGGAATTCTCAGGCCTCATGGGGTAG, which contain added *Nhe*I and *Eco*RI restriction sites, respectively. ΔTS-MetAP1D, which lacks the mitochondrial targeting sequence (residues 1−55), was subcloned with the following primers: forward, 5′-GCGGCTAGCGCTGCAGTTTCTTCAGCTC, and the full-length reverse primer. The N-terminal His-tag was separated from FL- and ΔTS-MetAP1D via a thrombin cleavage site in the vector backbone. Both constructs were transformed into BL21(DE3) *E. coli* cells (Stratagene) for protein expression. A 50 mL overnight culture was inoculated into 2 L of LB medium and incubated at 37 °C while shaking at 250 rpm. At $OD_{600} = 1.0$, the temperature was reduced to 16 °C and the culture, induced with 1 mM IPTG, was further incubated for 72 h while shaking at 150 rpm. Cells were harvested by centrifugation at 5000*g* and stored at −80 °C.

The frozen cell pellet was resuspended in phosphate buffer [50 mM NaH_2PO_4, 300 mM NaCl, and 10 mM imidazole, pH 8.0, with complete protease inhibitor cocktail (Roche, Indianapolis, IN)] and lysed by passing twice through a French press. All subsequent steps were conducted at 4 °C. Cell debris was cleared by centrifugation at 15 000 rpm for 60 min. The supernatant was loaded onto a Ni-NTA nickel affinity column (Qiagen). The protein purification was carried out according to the manufacturer's recommendations under

[1] Abbreviations: MetAP(1,2), methionine aminopeptidase (type 1 or 2); ProAP, proline aminopeptidase; *p*-NA, *p*-nitroaniline; RT-PCR, reverse transcriptase−polymerase chain reaction; ΔTS, deletion of mitochondrial targeting sequence; FL, full-length; HEPES, *N*-(2-hydroxyethyl)piperazine-*N*′-ethanesulfonic acid; IPTG, isopropyl β-D-thiogalactoside; MALDI-TOF, matrix-assisted laser desorption ionization time-of-flight.

[2] The terms metalloprotein and metalloenzyme are best reserved for proteins or enzymes that copurify together with their essential metal ions, implying a dissociation constant ≤ 10 nM; this is not the case with MetAPs, which bind their metal activators more weakly.

native conditions. Briefly, phosphate buffer was continuously used to wash the column until the absorption at 280 nm reached the baseline. The column was further washed with lysis buffer plus 20 mM imidazole and then lysis buffer plus 40 mM imidazole. The bound proteins were eluted with lysis buffer plus 75 mM imidazole before subsequent dialysis into storage buffer (25 mM HEPES, pH 8.0, 150 mM KCl, and 10% glycerol) in the presence of Chelex 100 (Bio-Rad). The protein was then concentrated by Amicon ultracentrifugal filter devices (Millipore), frozen in liquid nitrogen, and stored at −80 °C. Protein concentrations were determined by absorption at 280 nm with an estimated extinction coefficient of 28 608 M^{-1} cm^{-1} for the full-length protein and 27 118 M^{-1} cm^{-1} for the ΔTS protein. Both purification procedures yielded a total of 1 mg of pure protein (single band on the SDS−polyacrylamide gel) from a 4 L culture. Cleavage of the *N*-terminal His-tag was carried out with biotinylated thrombin from Novagen (San Diego, CA), and the residual biotin−thrombin was removed by streptavidin−agarose beads, according to the manufacturer's instructions.

The expression and purification of GST-tagged wild-type human MetAP1 and H212A and H212K mutants were conducted as described by Addlagatta et al. (*22*). Site-directed mutagenesis was performed with the QuikChange site-directed mutagenesis kit from Stratagene (La Jolla, CA) according to the manufacturer's instructions. The primers for the H212A mutant are (up) 5′-GAATGAAGTCATTTGCGCGGGAATACCAGACAGAAG and (down) 5′-CTTCTGTCTGGTATTCCCGCGCAAATGACTTCATTC. The primers for the H212K mutant are (up) 5′-GAATGAAGTCATTTGCAAAGGAATACCAGACAGAAG and (down) 5′-CTTCTGTCTGGTATTCCTTTGCAAATGACTTCATTC (the altered codons are underlined). Constructs were confirmed by DNA sequencing before transformation into BL21 cells for expression. The construct of *E. coli* MetAP was a generous gift from Dr. Brian W. Matthews' group, and the recombinant *E. coli* MetAP was purified as described by Lowther et al. (*31*). All of the proteins were dialyzed in storage buffer (25 mM HEPES, pH 8.0, 150 mM KCl, and 10% glycerol) in the presence of Chelex 100. The proteins were then concentrated as described above, frozen in liquid nitrogen, and stored at −80 °C.

MetAP Enzymatic Assay. The enzymatic assay was adapted from Zhou et al. (*32*) and was performed at 23 °C on a 96-well polystyrene microplate. All of the compounds were purchased from Sigma (St. Louis, MO) except where noted. Proline aminopeptidase (ProAP) was a generous gift from Dr. Brian W. Matthews. The reaction buffer solution (40 mM HEPES, pH 8.0, and 100 mM NaCl) and the substrate, Met-Pro-*p*-NA, were passed over a Chelex 100 column (10 × 1 cm) to remove all traces of contaminating metal ions. ProAP was treated with approximately 1 mL (wet bed volume) of Chelex 100 resin at 4 °C with periodic mixing. The resin was then separated by centrifugation in a conical tube and the supernatant protein solution was removed. In the kinetic studies of metal activation, each well contained a 100 μL mixture of 40 mM HEPES (pH 8.0), 100 mM NaCl, 3 mM Met-Pro-*p*-NA, 1 unit/mL ProAP, 0.4 μM FL- or ΔTS-MetAP1D and various concentrations of divalent metal ions ($CoCl_2$, $MnCl_2$, $NiCl_2$, $ZnCl_2$, $MgCl_2$, or $CaCl_2$) (Sigma, St. Louis, MO). EDTA, 1,10-phenanthroline, 1,7-phenanthroline and 2,6-pyridinedicarboxylic acid were purchased from Sigma. The production of *p*-NA was monitored continuously by the increasing absorbance at 405 nm ($\epsilon = 1.06 \times 10^4$ M^{-1} cm^{-1}). The initial rate of hydrolysis was determined from the early linear portion of the enzymatic reaction curve, by subtraction of the background spontaneous hydrolysis rate measured in the absence of MetAP1D. The incubation periods were adjusted in length to result in the utilization of ≤15% of the added substrate. The kinetic constants, K_m and k_{cat}, were determined by the same experimental procedures, and the data were fit to the Michaelis−Menten equation with GraphPad Prism 4 software (San Diego, CA).

pH studies. The enzymatic activity of ΔTS-MetAP1D was measured with Met-Pro-*p*-NA as the substrate. Apoenzyme (1 μM) was incubated with Co^{2+} at 23 °C for 10 min prior to reaction. All buffers were 40 mM with 100 mM NaCl. The buffers used were as follows: pH 5.0−5.5, sodium acetate; pH 6.0−7.0, Na^+-MES; pH 7.5−8.0, Na^+-HEPES; pH 8.5−9.0, Tris-HCl. The kinetic parameters at each pH value were determined by fitting the data to the Michaelis−Menten equation with GraphPad Prism 4 software.

Metal Activation Assay. All enzymes, buffer solutions, and substrates were treated with Chelex 100 (Bio-Rad) before each experiment (*33*). Each reaction contained a mixture of 40 mM Na^+-HEPES (pH 8.0), 100 mM NaCl, 3 mM Met-Pro-*p*-NA, and 1 unit/mL ProAP in a total volume of 100 μL. For the *E. coli* MetAP, 0.1 μM enzyme was used in each reaction. For the wild-type human MetAP1, 0.4 μM enzyme was used in each reaction. For the H212A and H212K mutants of human MetAP1, the mitochondrial FL- and ΔTS human MetAP1D, 1 μM protein was used in each reaction. The production of *p*-NA was monitored continuously by the increasing absorbance at 405 nm ($\epsilon = 1.06 \times 10^4$ M^{-1} cm^{-1}). The initial rate of hydrolysis was determined from the early linear portion of the enzymatic reaction curve, subtracting the background hydrolysis measured in the absence of the corresponding MetAP. The velocity was initially plotted against the total metal concentrations and fit to the Hill equation (eq 1):

$$E + nM \rightleftarrows EM_n \tag{1a}$$

$$(K_{0.5})^n = ([E]_{free}[M]_{free}{}^n)/[EM_n] \tag{1b}$$

to estimate the Hill coefficient (n) and the macroscopic dissociation constant ($K_{0.5}$) with GraphPad Prism 4 software (San Diego, CA). EM_n is assumed to be the kinetically active species. The resulting initial values of $K_{0.5}$ and n were used to calculate the free metal concentrations by fitting the data to eq 2, which is obtained from eqs 1, 3, and 4 by the mass conservation rules, and plotted against the corresponding velocity.

$$(K_{0.5})^n = \{([E]_{total} - [EM_n])([M]_{total} - n[EM_n])^n\}/[EM_n] \tag{2}$$

$$[M]_{total} = [M]_{free} + n[EM_n] \tag{3}$$

$$[E]_{total} = [E]_{free} + [EM_n] \quad (4)$$

Such a plot is fit again with the Hill equation (eq 1) to generate new $K_{0.5}$ and n values. This process was repeated until $K_{0.5}$ and n did not change by further iterations. Generally, no further changes in n or $K_{0.5}$ were found after five iterations.

Prediction of Mitochondrial Targeting Sequence. A multilayer classifier system, Protein Prowler 1.2 (*34*), was used to predict the mitochondrial targeting sequence in human MetAP1D. Sequences from human MetAP1D (AY374142) and *E. coli* MetAP (NP_285862) were aligned by ClustalW (*35*) from http://www.ebi.ac.uk/clustalw/ and Blast (*36*) from http://www.ncbi.nlm.nih.gov/blast/ to compare the overall sequence homology and the conservation of specific residues.

Circular Dichroic Spectroscopy. Far-UV CD spectra were collected between 200 and 280 nm on an Aviv 62A DS spectropolarimeter in a 0.1 cm cuvette at 23 °C. Spectra were accumulated by scanning four times at a scan rate of 20 nm/min. The baseline offset was corrected by subtracting the readings from buffer alone [20 mM Tris (pH 8.0) and 100 mM NaCl]. Protein concentrations ranged from 12 to 18 μM. The ellipticity is reported as the mean residue ellipticity, θ (in units of degrees centimeter^2 decimole^{-1} residue^{-1}). The fractions of helix, β-structure, and random coil were computed by using the *k2d* program based on Kohonen neural network calculations (*37*, *38*).

Determination of Molecular Weight by Mass Spectrometry. Purified proteins were dissolved in 20 mM Tris (pH 8.0) to a final concentration of 10 μM. The samples were subjected to MALDI-TOF mass spectrometry by using a Voyager-DE STR mass spectrometer. Aldolase (Sigma), MW 39 212.28, was used as the standard molecular weight marker.

Metal Analysis. Purified proteins, after removal of the His-tag by on-column thrombin digestion, were diluted in Chelex-100-treated buffer (10 mM Tris-HCl, pH 8.0) to a final concentration of 2.5 μM. Concentrations of metal ions were determined by standard inductively coupled plasma (ICP) emission analysis (*39*) at the Chemical Analysis Laboratory, University of Georgia, 110 Riverhead Rd., Athens, GA 30602-4695, and corrected by buffer alone. Data were expressed as micromolar metal/micromolar protein.

RESULTS

Recombinant Expression of Full-Length and Targeting-Sequence-Deletion (ΔTS) Human MetAP1D. To facilitate the characterization of the newly reported human mitochondrial MetAP1D, we cloned the cDNA according to the open reading frame (ORF) sequence in the GenBank database (*16*). An expression plasmid was constructed for the full-length MetAP1D to be expressed as a fusion protein with an N-terminal hexa-His-tag. A thrombin cleavage site was placed between the His-tag and the MetAP1D ORF. Although the His-tagged full-length MetAP1D fusion protein was expressed upon IPTG induction, most of it was insoluble when *E. coli* cells were grown at 37 °C. The insolubility problem was solved by growing the bacteria at 16 °C upon IPTG induction. The recombinant His-tagged full-length MetAP1D fusion protein was purified by use of Ni-NTA Superflow resins. Thrombin treatment released the full-length MetAP1D from the fusion protein (Figure 1).

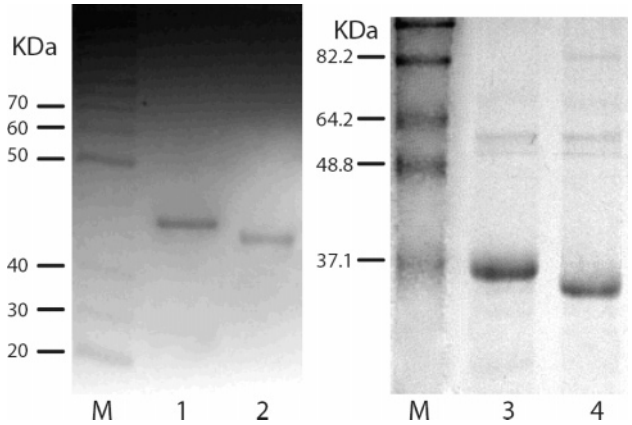

FIGURE 1: Recombinant proteins of full-length MetAP1D and ΔTS-MetAP1D resolved from SDS−polyacrylamide gel. Lane 1, purified His-tagged FL-MetAP1D (2 μg of protein loaded); lane 2, purified FL- MetAP1D with His-tag removed by thrombin cleavage (1 μg of protein loaded); lane 3, purified His-tagged ΔTS-MetAP1D (4 μg of protein loaded); lane 4, purified ΔTS-MetAP1D with His-tag removed by thrombin cleavage (3 μg of protein loaded). M, protein markers.

Table 1: Total Metal Ion Amount[a] after Purification

metal	FL-MetAP1D	ΔTS-MetAP1D
Ca	<0.01	0
Cd	0.04	0.04
Co	<0.01	<0.01
Cr	<0.02	<0.03
Cu	0.05	0.10
Fe	0.07	0.09
Mg	<0.1	<0.2
Mn	0	0
Mo	0	0
Ni	0.2	0.2
Si	0.6	0.7
Sr	0	0
Zn	0.04	0.05

[a] Micromolar metal/micromolar MetAP1D.

Previous studies suggested that MetAP1D contains an N-terminal targeting sequence for mitochondria (*16*). By use of a multilayer classifier system, Protein Prowler 1.2 (*34*), the first 55 amino acids were predicted as the mitochondrial targeting sequence. A targeting-sequence-deletion mutant (ΔTS) lacking residues 1−55 was constructed with an *N*-terminal hexa-His-tag and a thrombin cleavage site between the His-tag and Ala 56 of MetAP1D. The recombinant fusion protein was expressed in *E. coli* at 16 °C before purification on Ni-NTA resins. The predicted molecular weight for the His-tagged ΔTS-MetAP1D was 33 091.1 Da, and the value obtained by MALDI-TOF mass spectroscopy was 33 132.4 Da. Thrombin cleavage was able to release ΔTS MetAP1D from the fusion protein (Figure 1). The predicted and observed molecular weights were 31 209.0 and 31 229.6 Da, respectively.

Divalent Cations Are Required To Activate MetAP1D. Methionine aminopeptidases are known to be metal-activated proteases (*6*). Sequence alignments between human MetAP1D and other MetAP family members have confirmed the conservation of the metal-coordinating residues. As shown in Table 1, trace metal analysis of FL- and ΔTS-MetAP1D revealed negligible levels of Ca, Co, Cr, Mg, Mn, Mo, and Sr. Trace amounts of Cd, Cu, Fe, Ni, Si, and Zn were detected. The slightly higher levels of Ni (0.2 μM/μM

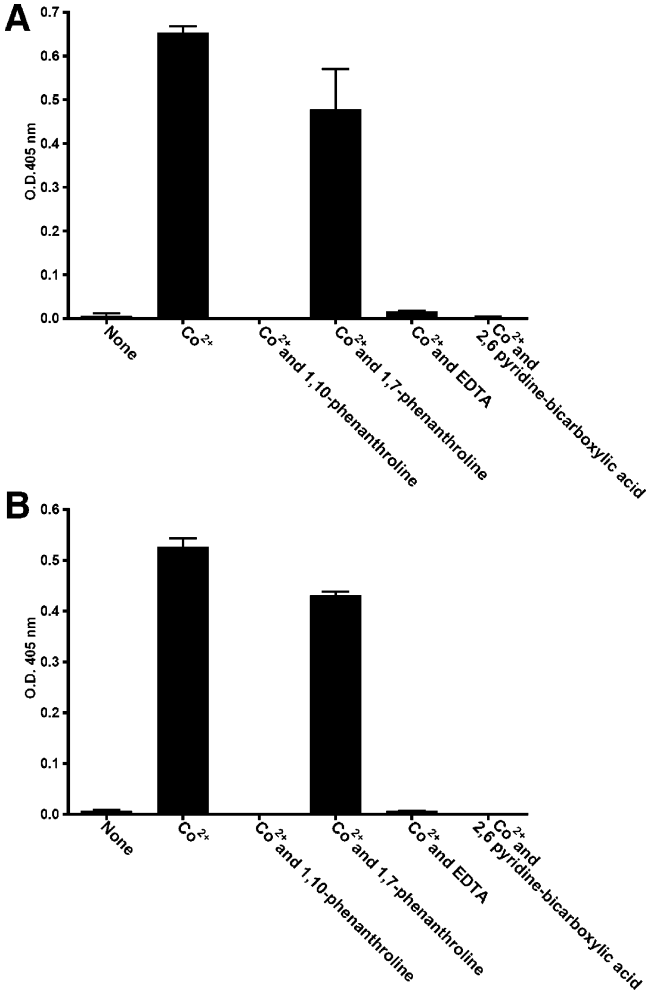

FIGURE 2: Metal dependence for activation of (A) full-length MetAP1D and (B) ΔTS-MetAP1D, tested in the absence and presence of 10 μM divalent cobalt (Co^{2+}) ions. Chelating agents 1,10-phenanthroline (100 μM), EDTA (100 μM), and 2,6-pyridinedicarboxylic acid (100 μM) were added in addition to the metal ions. 1,7-Phenanthroline (100 μM) is shown as a negative control. All rates have been corrected for background rates measured in the absence of enzyme as a result of spontaneous hydrolysis of the substrate. Bars labeled None show the error levels in the background-corrected rates. Error bars represent 1 standard deviation from triplicate measurements.

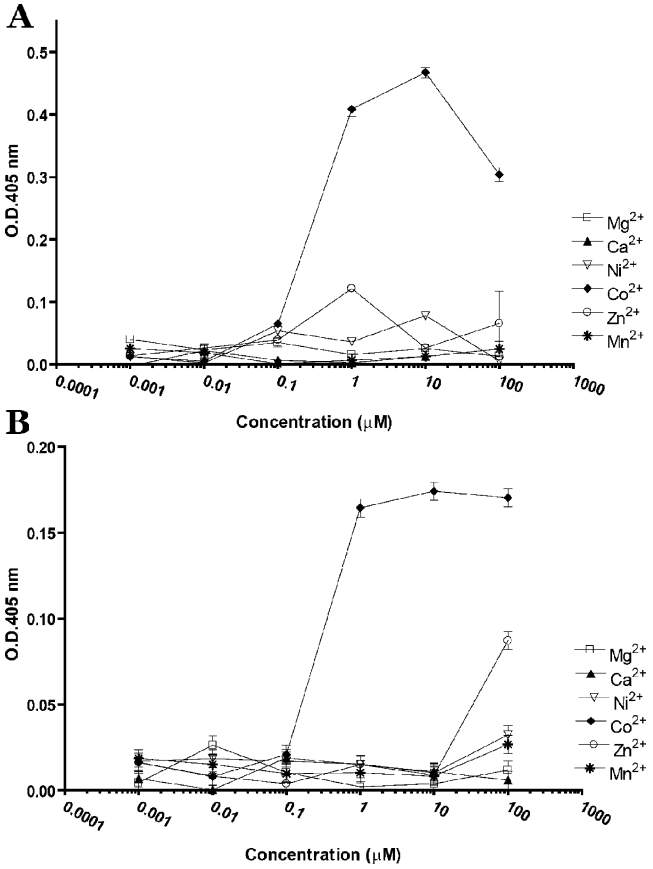

FIGURE 3: Activation of (A) full-length MetAP1D and (B) ΔTS-MetAP1D by divalent metal ions, tested with fixed substrate concentration (2 mM) in the presence of various concentrations of divalent metal ions. Error bars represent 1 standard deviation from triplicate measurements.

protein) likely came from the Ni resin used for enzyme purification. To explore the metal ion requirement for MetAP1D, we used a proline aminopeptidase (ProAP) -coupled enzymatic assay (*32*) to study the metal-dependent hydrolysis of Met-Pro-*p*-nitroanilide by FL- and ΔTS-MetAP1D, respectively. As shown in Figure 2, the processing of the methionine-containing substrate remained at the background level observed in the absence of MetAP, when metal ions were not added to the enzymatic assay. However, the addition of divalent cobalt ions (Co^{2+}) significantly stimulated the activities of the FL- and ΔTS-MetAP1D enzymes. Such stimulations were quenched to background level in the presence of metal chelators, for example, EDTA, 1,10-phenanthroline, and 2,6-pyridinedicarboxylic acid, but much less so by 1,7-phenanthroline, an isomer of 1,10-phenanthroline with no metal-chelating ability (Figure 2).[3]

[3] The slight inhibition by 1,7-phenanthroline may result from its weak hydrophobic binding with the active site.

These observations indicated that MetAP1D is a member of the MetAP metal-activated protease family.[2]

Although MetAPs have been studied as metal-activated proteases, the physiological metal for this family of enzymes remains to be defined (*18*, *40*−*42*). Previous reports have demonstrated that, in addition to Co^{2+}, a few other divalent metal ions are also capable of activating this family of enzymes in vitro (*43*, *44*). As shown in Figure 3, both full-length MetAP1D and ΔTS-MetAP1D were significantly activated by Co^{2+}. At high concentrations (100 μM), Co^{2+} appeared to be inhibitory to the full-length enzyme. Zn^{2+} was found to activate full-length MetAP1D slightly (at ∼1 μM) and ΔTS-MetAP1D (at 100 μM), while other divalent metal ions were ineffective. These results indicate that Co^{2+} is by far the best activator of MetAP1D in vitro and likely its required activator in vivo.

Kinetic Properties of MetAP1D. By kinetic analysis, optimal enzymatic activity of ΔTS-MetAP1D in the presence of Co^{2+} was found to occur over the narrow pH range between 7.5 and 8.0 (Figure 4), similar to the pH profile on V_{max} of *E. coli* MetAP (*45*). While the K_m of Met-Pro-*p*-NA with ΔTS-MetAP1D at pH 8.0 was comparable to that for human cytosolic MetAP1, the k_{cat} was 66-fold lower (Table 2). Moreover, in comparison with *E. coli* MetAP, the k_{cat} of ΔTS-MetAP1D was 280-fold lower, and the K_m was 3-fold greater (Table 2). These differences did not result from the deletion of the targeting sequence since full-length MetAP1D showed similar kinetic parameters ($K_m = 573 \pm 45$ μM; k_{cat}

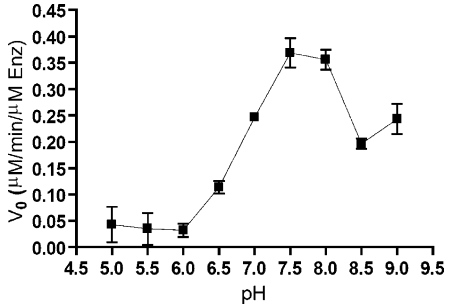

FIGURE 4: pH dependence of maximal activity for ΔTS-MetAP1D: plot of V_{max} versus pH. The assays were performed with 3 mM Met-Pro-*p*-NA as substrate. Co^{2+} concentration in the assay was 10 μM; other components are given in the text. Error bars represent 1 standard deviation from triplicate measurements.

Table 2: Kinetic Parameters for Methionine Aminopeptidases[a]

MetAP	n (Co^{2+})	$K_{0.5}$ (Co^{2+}) (μM)	k_{cat} (min^{-1})	K_m (substrate) (μM)
E. coli	2.1 ± 0.2	0.2 ± 0.02	109 ± 10	180 ± 20
human type 1D/ΔTS	1.8 ± 0.2	0.42 ± 0.05	0.4 ± 0.1	588 ± 72
human type 1D (His-tag)/ΔTS	2.0 ± 0.2	0.37 ± 0.04	0.37 ± 0.03	564 ± 58
human type 1 WT	2.9 ± 0.2	0.26 ± 0.03	25.5 ± 0.9	740 ± 80
H212A	2.2 ± 0.2	1.7 ± 0.2	0.42 ± 0.01	270 ± 37
H212K	1.4 ± 0.1	41 ± 4.0	0.014 ± 0.002	787 ± 56

[a] Hill coefficients (n) and macroscopic dissociation constants ($K_{0.5}$), k_{cat}, and K_m values were determined by the ProAP-coupled assay with Met-Pro-*p*-nitroanilide as substrate (*31*). Errors represent 1 standard deviation.

$= 0.42 \pm 0.06\ min^{-1}$). Human MetAP1D is 61% homologous to *E. coli* MetAP and gave a CD spectrum nearly identical to that of the *E. coli* MetAP (Figure 5), suggesting that they are likely to have very similar secondary structures. The X-ray structure of the *E. coli* MetAP-Co^{2+} complex has 27.4% helix, 21.3% β-structure, and 51.3% coil (*18*). Analysis of the CD spectra (Table 3) confirms very similar and presumably intact secondary structures of *E. coli* MetAP, FL-MetAP1D, and ΔTS-MetAP1D. Hence human mitochondrial MetAP1D is a less efficient catalyst than human cytosolic MetAP1 or *E. coli* MetAP under the present assay conditions in vitro.

Activation of ΔTS-MetAP1D by Co^{2+}. To further investigate the metal activation of recombinant MetAP1D, we performed steady-state kinetic analyses on ΔTS-MetAP1D because the targeting sequence is removed in vivo after the full-length protein is transported into mitochondria (*46*). At saturating substrate concentrations, a plot of velocity versus free Co^{2+} concentration showed sigmoidal metal activation, both with (Figure 6A) and without (Figure 6B) the His-tag. Fitting these data to the Hill equation (eq 1) (*29*) yielded a Hill coefficient (n) of 2.0 ± 0.2 and a $K_{0.5}$ of 0.37 ± 0.04 μM for His-tagged ΔTS-MetAP1D, and indistinguishable values of $n = 1.8 \pm 0.2$ and $K_{0.5} = 0.42 \pm 0.04$ μM for non-His-tagged ΔTS-MetAP1D (Table 2). These results indicate the binding of at least two Co^{2+} ions in the activation of MetAP1D, which may or may not be cooperative, and indicate that the His-tag is not interfering with the metal-binding properties of this enzyme.

Activation of E. coli and Human MetAP1 by Co^{2+}. Previous observations that Co^{2+} maximally stimulated *E. coli* MetAP have suggested that this family of enzymes preferentially utilize Co^{2+} in vivo (*4*, *47*). X-ray structural studies of EcMetAP have demonstrated two metal-binding sites, with each metal ion sharing one Glu, one Asp, and one water

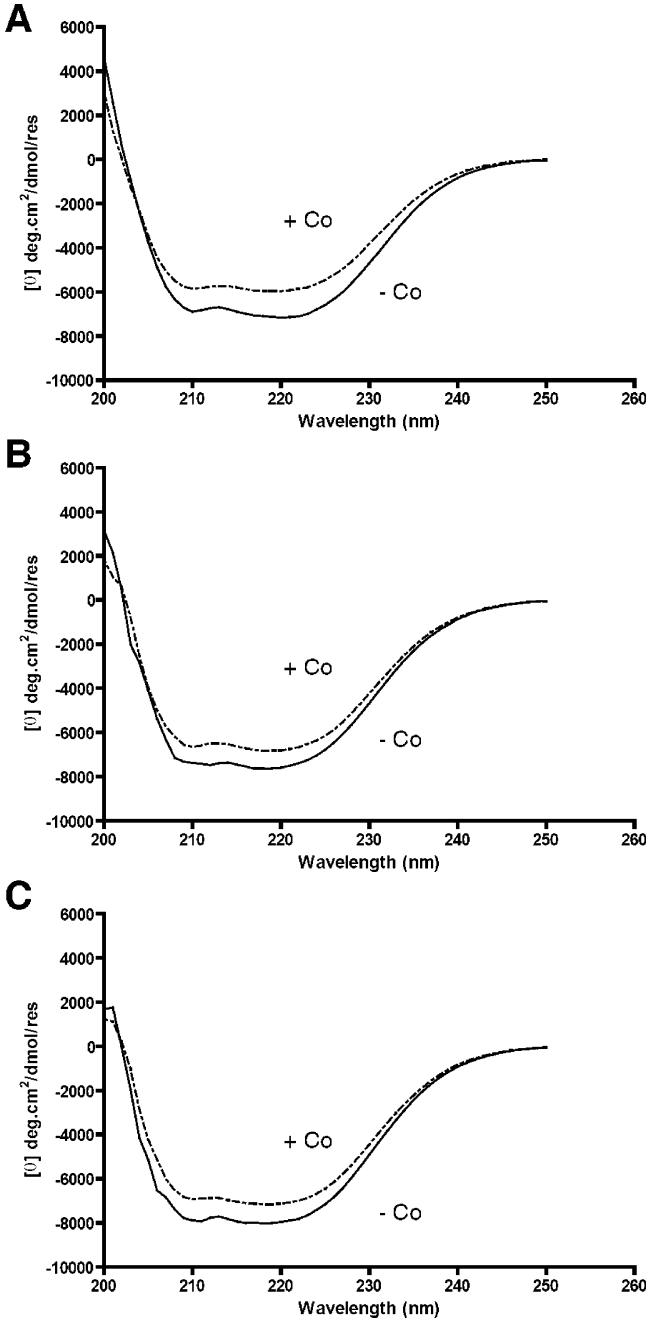

FIGURE 5: Far-UV circular dichroic spectra of (A) apo-EcMetAP, (B) apo-full-length MetAP1D (FL-MetAP1D), and (C) apo-ΔTS-MetAP1D with or without $CoCl_2$ (molar ratio of protein:cobalt is 1:3). Conditions: 20 mM Tris (pH 8.0) and 100 mM NaCl at 23 °C. (—) Apoenzyme; (---) Co^{2+}-charged enzyme.

Table 3: Estimation of the Fractions of Protein Secondary Structure from UV Circular Dichroism Spectra[a]

	helix	β-structure	random coil
EcMetAP (apo)	0.31	0.18	0.52
EcMetAP (Co)	0.28	0.20	0.52
FL-MetAP1D (apo)	0.31	0.16	0.53
FL-MetAP1D (Co)	0.29	0.18	0.53
ΔTS-MetAP1D (apo)	0.31	0.15	0.54
ΔTS-MetAP1D (Co)	0.30	0.16	0.54

[a] By use of the *k2d* Program.

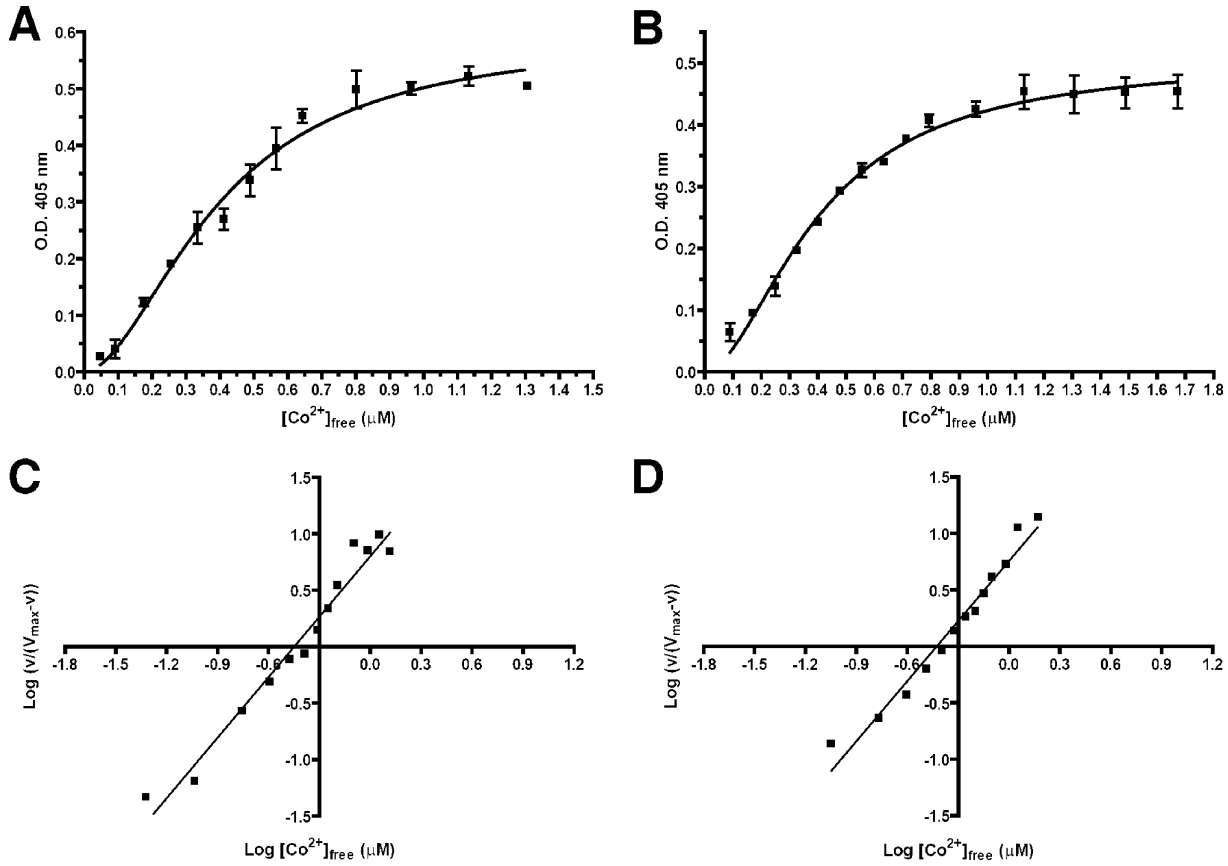

FIGURE 6: ΔTS-MetAP1D activation by Co^{2+}. Specific activities at saturating substrate of (A) His-tagged ΔTS-MetAP1D and (B) non-His-tagged ΔTS-MetAP1D are plotted versus free Co^{2+} concentrations. Hill plots (*29*) for (C) His-tagged ΔTS-MetAP1D and (D) non-His-tagged ΔTS-MetAP1D utilize a form of the Hill equation that may be extended to kinetic measurements [i.e., $\log (v/(V_{max} - v)) = n \log [M] - \log K_{0.5}$, where v = velocity, V_{max} = maximum velocity, and $K_{0.5}$ = macroscopic equilibrium constant]. Solid lines result from linear regression analysis. The parameters from the Hill plot fitting agree with those from the sigmoidal regression fitting. Hill coefficients (n) and $K_{0.5}$ values are summarized in Table 2. Error bars represent 1 standard deviation from triplicate measurements.

ligand (*18*). Additional Glu, Asp, and His residues serve as unshared metal ligands. These five metal-coordinating residues have been conserved in MetAP family members throughout evolution from prokaryotes to humans (*4*). However, some studies of *E. coli* MetAP claim the activation of this enzyme by only one divalent cation (*24*, *48*). Moreover, although all of the metal-coordinating residues are conserved in human MetAP1 and this enzyme is activated by Co^{2+} in vitro, X-ray structural studies of human MetAP1 have detected a third metal-binding site in the active pocket (*22*).

These observations have raised questions about how many metal ions are required for maximal activation of *E. coli* MetAP and human cytosolic MetAP1, respectively. At saturating substrate concentrations, the plots of velocity versus free Co^{2+} showed sigmoidal metal activation of *E. coli* MetAP (Figure 7A) and human MetAP1 (Figure 7B). Fitting the data to the Hill equation (eq 1) yielded Hill coefficients (n) of 2.1 for *E. coli* MetAP and 2.9 for human MetAP1, respectively (Table 2). These results indicate that *E. coli* MetAP requires at least two cobalt ions for maximal activation, while human cytosolic MetAP1 requires at least three, in accord with the X-ray structures of these enzymes (*17*, *21*).

Since His212 is a conserved residue that coordinates only the third Co^{2+} ion in the crystal structure of human MetAP1, we generated two mutant proteins by site-directed mutagenesis, H212A and H212K, to further explore possible activation of MetAP1 by the third metal ion. Recombinant mutant proteins were expressed and purified from *E. coli*. Fitting the plot of velocity versus free Co^{2+} to eq 1 yielded decreased values of $n = 2.2$ for H212A (Figure 7C) and $n = 1.4$ for H212K (Figure 7D), respectively. The average dissociation constants ($K_{0.5}$) of Co^{2+} from H212A and H212K increased 6- and 157-fold, respectively, and k_{cat} decreased 60- and 1800-fold, respectively, in comparison with the wild-type enzyme (Table 2). These results indicate that His212 is essential for the activation of human MetAP1 by the third metal ion, which contributes significantly to catalysis.

DISCUSSION

The processing of the initiator methionine from nascent polypeptides is a modification that has been found to be essential for about two-thirds of the proteins of various proteomes (*6*, *49*, *50*). Methionine aminopeptidases have been shown to be involved in this process in all of the organisms studied. In addition to the two isoforms of MetAP in eukaryotic cells conserved from yeast to humans, a third isoform has recently been identified in human cells, namely, MetAP1D, which is localized in the mitochondria (*16*). Downregulation of MetAP1D expression in HCT-116 colon carcinoma cells suggested an important function in colon oncogenesis (*17*). Our expression and purification of the recombinant FL- and ΔTS-MetAP1D proteins have facilitated the kinetic characterization of this enzyme. The observations that MetAP1D activity is stimulated by the

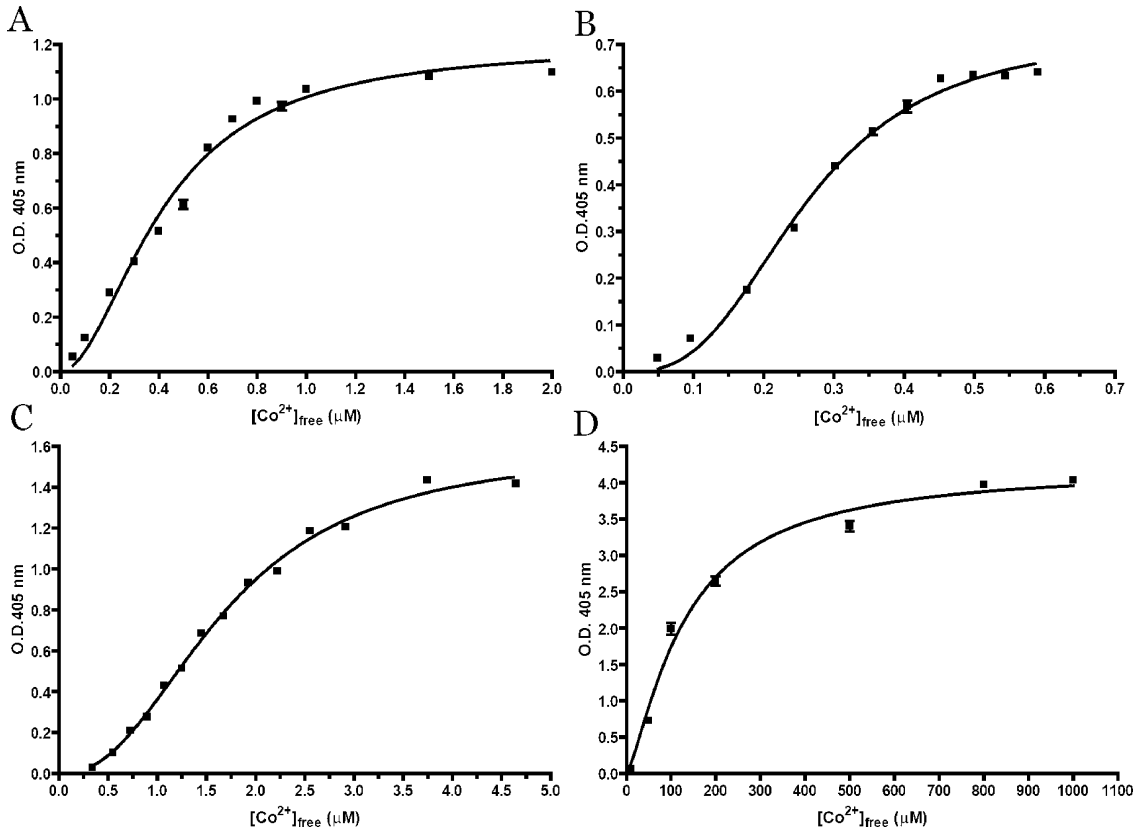

FIGURE 7: *E. coli* MetAP and human MetAP1 activation by Co^{2+}. Specific activities at saturating substrate of (A) *E. coli* MetAP, (B) human MetAP1 wild type, (C) human MetAP1 H212A, and (D) human MetAP1 H212K are plotted versus free Co^{2+} concentrations. The plots were fitted by the Hill equation (eq 1). Hill coefficients (n) and $K_{0.5}$ values are summarized in Table 2. Error bars represent 1 standard deviation from triplicate measurements.

addition of divalent metal ions (Co^{2+}) and is inhibited by metal chelating agents indicate that MetAP1D is a metal-activated protease (Figure 2).[2] Comparison of various divalent metal ions has indicated that Co^{2+} is by far the best, and hence the likely physiologically relevant, activator of human MetAP1D (Figure 3).

The k_{cat} values reveal that the recombinant human MetAP1D is 280-fold less efficient a catalyst than *E. coli* MetAP and 66-fold less efficient than human MetAP1 (Table 2). It is possible that Met-Pro-*p*-NA is not the optimal substrate for MetAP1D despite the fact that three mitochondrially encoded proteins which are likely substrates for MetAP1D contain Met-Pro- at their amino termini (*50*). A comparative assay with the substrate Met-Ala-Ser showed human MetAP1D to be significantly less active than human MetAP1 and comparable in activity to human MetAP2 (*16*). Although MetAP1D is 61% homologous to *E. coli* MetAP, containing all of the five conserved metal-liganding residues and showing very similar secondary structure to the *E. coli* enzyme by CD spectroscopy (Figure 5, Table 3), it remains possible that human MetAP1D is missing one or more important residues that contribute to enzyme catalysis. While the human mitochondrial genome encodes only 13 proteins, which constitute the substrate pool of human MetAP1D (*51*), the lower catalytic activity of MetAP1D apparently is kinetically and biologically competent in this specialized compartment. Indeed, the low activity of mitochondrial MetAP1D may be biologically necessary to minimize inappropriate hydrolytic events. By analogy, intracellular proteases are usually in the form of inactive zymogens (*52*), and intracellular nucleases, such as the 3′,5′-exonuclease of DNA polymerase 1, are low in activity (*53*).

By using a functional assay of velocity versus free Co^{2+}, we have observed sigmoidal metal binding to, and activation of, MetAP1D. The Hill coefficient (n) indicates that at least two Co^{2+} ions are required for maximal MetAP1D activation (Table 2). This is probably not the result of contamination by a chelating agent (e.g., EDTA) because the Chelex 100 chelating resin, rather than EDTA, was used for the removal of trace metals from all solutions (Table 1). Our results also reveal that *E. coli* MetAP requires at least two Co^{2+} ions for maximal activation, consistent with the X-ray structure, which revealed a binuclear Co^{2+} complex (*18*). We note that these results differ from those of other studies which claimed that *E. coli* MetAP requires only one divalent cation for full activity (*24*, *45*). We have reanalyzed the data from Ye et al. (*24*) that show velocity as a function of total Co^{2+} concentration. Fitting these data to eq 1 yields a Hill coefficient (n) of 2.1 ± 0.2, and iteration of these data to calculate free Co^{2+} yields n values significantly greater than 2, possibly due to enzyme aggregation at the high protein concentrations (20 μM) used by Ye et al. (*24*). Reanalysis of the data from Copik et al. (*45*) that show velocity as a function of free Fe^{2+} by use of eq 1 yields a Hill coefficient of 0.8 ± 0.08. While metal activation by Fe^{2+} may differ from that with Co^{2+}, the small number of rate measurements at low metal concentrations do not exclude sigmoidal behavior (*45*).

A titration of *E. coli* MetAP with Co^{2+}, in the absence of substrate, monitored by atomic absorption spectrometry and

magnetic circular dichroism detected 1.1 Co^{2+} binding sites but two ground-state geometries for bound Co^{2+}, a fully populated pentacoordinate site and a ~10% populated octahedral site (*54*). The Hill coefficient (*n*) for Co^{2+} binding of 1.3 ± 0.2 was interpreted as showing slight cooperativity in forming a binuclear enzyme−$(Co^{2+})_2$ complex (*54*). Our kinetic data suggest that the presence of saturating substrate may increase the cooperativity of Co^{2+} binding to *E. coli* MetAP, raising the Hill coefficient to 2.1 ± 0.2 (Table 2).

With human cytosolic MetAP1, our kinetically determined Hill coefficient of 2.9 (Table 2) indicates that the wild-type enzyme binds at least three Co^{2+} ions for maximal activation. The results of this functional assay are consistent with the X-ray structure of this enzyme, which shows a third Co^{2+} ion coordinated primarily by the conserved residue His212 (*22*). To examine the function of the third Co^{2+} in the active site of human MetAP1, we generated two mutants, H212A and H212K. Kinetic studies (Table 2) show no increases in the K_m of the substrate but marked 60- and 1800-fold decreases in k_{cat} with H212A and H212K, respectively. Significant decreases in the Hill coefficients for Co^{2+} activation (*n*) to values of 2.2 and 1.4 for H212A and H212K, respectively, indicate that the side chain of His 212 is important for coordinating the third Co^{2+} ion, which may cooperatively contribute to maximal enzyme activation. The 6.5- and 158-fold increases in the $K_{0.5}$ values of Co^{2+} with the H212A and H212K mutants, respectively, may also reflect a decrease in cooperativity, and the absence of an increase in the K_m value of the substrate suggests that these mutations do not weaken substrate binding. The observation that the H212K mutation is much more damaging to both Co^{2+} binding ($K_{0.5}$), and catalysis (k_{cat}) suggests that the positively charged side chain of Lys212 may directly compete with Co^{2+} for the third metal-binding site.

Activation of enzymatic catalysis by the third Co^{2+} ($Co^{2+}3$) may be direct or indirect. A reasonable and direct catalytic role for the third Co^{2+} ($Co^{2+}3$) would be that of an oxyanion hole, namely, an electrophile to polarize the carbonyl group of the methionyl-substrate, thereby facilitating the attack by a water-derived nucleophile, O_N. In the 1.1 Å X-ray structure of the trimetal complex of human MetAP1, $Co^{2+}3$ (at 50% occupancy) is coordinated not only by His212-Nϵ but also by a Cl^- anion (2.31 Å). This Cl^- closely approaches the likely water nucleophile O_N (2.12 Å), which is a shared ligand of both $Co^{2+}1$ and $Co^{2+}2$ (Figure 8A). In our modeling, replacing the Cl^- ligand of $Co^{2+}3$ by the carbonyl oxygen of a methionyl substrate would, with minor adjustments, permit the water nucleophile O_N to directly contact (3.2 Å) the carbonyl carbon of the methionyl-substrate (Figure 8B). The oxyanion hole may also contain other electrophiles such as His310, which is positioned to donate a hydrogen bond (3.07 Å) to the Cl^-, and presumably to the carbonyl oxygen of the substrate (*22*).

A more remote candidate for the binding site of $Co^{2+}3$ is found in the 1.1 Å X-ray structure of human MetAP1, in which His212 has been covalently modified by the epoxide inhibitor ovalicin (*55*). In this structure, a third Co^{2+} is detected with full occupancy, at a site 11.4 Å from $Co^{2+}1$ and 12.8 Å from $Co^{2+}2$. This third Co^{2+} is coordinated by Glu128 (2.4 Å), Tyr195 (2.0 Å), and His310 (2.2 Å), which has been displaced from the active site by the inhibitor. This Co^{2+} is positioned where it might interact with residue 3 of

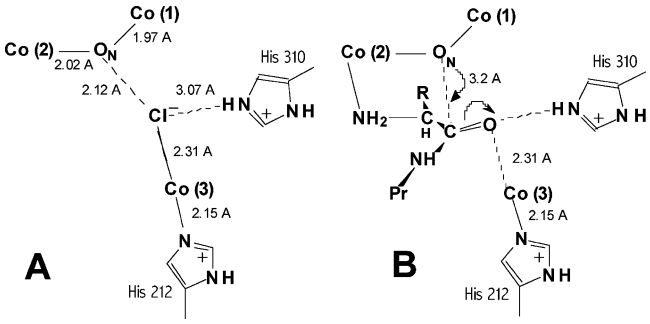

FIGURE 8: Proposed role of $Co^{2+}3$ as the oxyanion hole in the mechanism of human cytosolic MetAP1. (A) Arrangement of three Co^{2+} ions, His 212, the nucleophilic oxygen O_N, and a presumed Cl^- ligand at the active site of human cytosolic MetAP1, from the 1.1 Å X-ray structure of the trimetal enzyme (*22*). (B) Nucleophilic attack step in the mechanism of MetAP1, consistent with the present results, derived by replacing the Cl^- ligand of $Co^{2+}3$ by the carbonyl oxygen of methionyl-1 of a protein substrate (Pr), and positioning the carbonyl carbon in molecular contact (3.2 Å) with the nucleophilic oxygen O_N. The nucleophile is either hydroxide or oxide as discussed in the text.

the substrate to activate the leaving group. However, this third Co^{2+} binding site is not seen in the unmodified enzyme, in which His310 remains in the active site. Mutagenesis studies of the *E. coli* MetAP show that both His212 and His310 contribute significantly to catalysis (*56*). Of course, indirect activation of human MetAP1 by $Co^{2+}3$ could also occur, resulting from improved organization and stabilization of the active site.

That human MetAP1 requires a third metal ion for catalysis in comparison to *E. coli* MetAP and human MetAP2 has important implications on the future design and development of isoform-specific inhibitors of human MetAP1 as potential anti-cancer agents (*15*, *42*). Among the newly discovered MetAP1 inhibitors, a few have been shown to interact with the third metal ion that remains coordinated to His212 in MetAP1. Given the critical role of this third metal ion in catalysis by MetAP1, it is not surprising that these inhibitors bind to MetAP1 by partly forming liganding interactions with the third metal ion. It is interesting to note that although only two metal ions have been seen in the structures of *E. coli* MetAP, the third metal ion was seen in complexes between the *E. coli* enzyme and several of its inhibitors (*25*, *57*). Our kinetic analysis clearly indicates that at least two metal ions are required for optimal activity of *E. coli* MetAP. Thus, the third metal ion seen in structures of enzyme−inhibitor complexes of the bacterial enzyme is likely brought in by the metal coordinating inhibitor. In contrast, the third metal binding site in human MetAP1, which is partially occupied (*22*), is likely to become more fully occupied in the presence of the substrate. The existence of the third metal ion can be further exploited for the development of isoform-specific inhibitors of the MetAP1 subgroup of MetAP enzymes.

CONCLUSIONS

Expression and purification from *E. coli* of the recombinant human MetAP1D have made it possible to characterize the kinetic properties of this mitochondrial-targeted protein. Our studies establish that human mitochondrial MetAP1D is a metal-activated protease with Co^{2+} as the best activator. Functional kinetic studies indicate that at least two Co^{2+} ions

bind, with possible cooperativity, to maximally activate this enzyme as well as *E. coli* MetAP, consistent with the X-ray structure of the *E. coli* enzyme, which shows a binuclear Co^{2+} complex at the active site (*18*). Similarly, functional kinetic studies indicate that at least three Co^{2+} ions bind with possible cooperativity to maximally activate human cytosolic MetAP1, consistent with its X-ray structure, which shows a trinuclear Co^{2+} complex at the active site (*22*). In all of the MetAPs studied here, the simultaneous coordination of the attacking water by two Co^{2+} ions would facilitate its deprotonation to form a more nucleophilic species, hydroxide or oxide, thereby promoting catalysis (*2*, *5*). In the human cytosolic MetAP1, binding of the third essential Co^{2+} ion might activate the enzyme directly by serving as an oxyanion hole (Figure 8), together with His310 or indirectly by better organizing or stabilizing the structure at the active site, as indicated by the marked decreases in both sigmoidicity of Co^{2+} binding and in catalysis on mutating His212, a major ligand of the third Co^{2+} ion. Moreover, distinct substrate specificities have been observed between hMetAP1 and hMetAP2 (*58*). It is possible that the unique presence of the third metal ion in the active site of hMetAP1 may also help to define its substrate specificity.

ACKNOWLEDGMENT

We are grateful to Drs. Anthony Addlagatta and Brian W. Matthews at the University of Oregon for providing us with the *E. coli* MetAP construct and the purified ProAP and for helpful discussions. We appreciate the Liu lab members Drs. Fan Pan, Woon-Kai Low, and Shrida Bhat for their help in cloning, enzyme purification, MALDI-TOF mass spectroscopy, and insightful discussions. We thank Ellen Kloss and Dr. Douglas Barrick for help with CD spectroscopy. We thank Dr. Theresa Shapiro from the Department of Pharmacology and Molecular Sciences for making available the SpectraMax microplate reader. We thank Dr. Sandra B. Gabelli of the Biophysics and Biophysical Chemistry Department for help with computer graphics.

REFERENCES

1. Sträter, N., Lipscomb, W. N., Klabunde, T., and Krebs, B. (1996) Two-Metal Ion Catalysis in Enzymatic Acyl- and Phosphoryl-Transfer Reactions, *Angew. Chem., Int. Ed Engl. 35*, 2024−2055.
2. Mildvan, A. S., Xia, Z., Azurmendi, H. F., Saraswat, V., Legler, P. M., Massiah, M. A., Gabelli, S. B., Bianchet, M. A., Kang, L. W., and Amzel, L. M. (2005) Structures and mechanisms of Nudix hydrolases, *Arch. Biochem. Biophys. 433*, 129−143.
3. De Paola, C. C., Bennett, B., Holz, R. C., Ringe, D., and Petsko, G. A. (1999) 1-Butaneboronic acid binding to *Aeromonas proteolytica* aminopeptidase: a case of arrested development, *Biochemistry 38*, 9048−9053.
4. Lowther, W. T., and Matthews, B. W. (2002) Metalloaminopeptidases: common functional themes in disparate structural surroundings, *Chem. Rev. 102*, 4581−4608.
5. Williams, N. H., Takasaki, B., Wall, M., and Chin, J. (1999) Structure and Nuclease Activity of Simple Dinuclear Metal Complexes: Quantitative Dissection of the Role of Metal Ions, *Acc. Chem. Res. 32*, 485−493.
6. Lowther, W. T., and Matthews, B. W. (2000) Structure and function of the methionine aminopeptidases, *Biochim. Biophys. Acta 1477*, 157−167.
7. Chang, S. Y., McGary, E. C., and Chang, S. (1989) Methionine aminopeptidase gene of *Escherichia coli* is essential for cell growth, *J. Bacteriol. 171*, 4071−4072.
8. Miller, C. G., Strauch, K. L., Kukral, A. M., Miller, J. L., Wingfield, P. T., Mazzei, G. J., Werlen, R. C., Graber, P., and Movva, N. R. (1987) N-terminal methionine-specific peptidase in *Salmonella typhimurium*, *Proc. Natl. Acad. Sci. U.S.A. 84*, 2718−2722.
9. Li, X., and Chang, Y. H. (1995) Amino-terminal protein processing in *Saccharomyces cerevisiae* is an essential function that requires two distinct methionine aminopeptidases, *Proc. Natl. Acad. Sci. U.S.A. 92*, 12357−12361.
10. Bradshaw, R. A., Brickey, W. W., and Walker, K. W. (1998) N-terminal processing: the methionine aminopeptidase and N alpha-acetyl transferase families, *Trends Biochem. Sci. 23*, 263−267.
11. Griffith, E. C., Su, Z., Turk, B. E., Chen, S., Chang, Y. H., Wu, Z., Biemann, K., and Liu, J. O. (1997) Methionine aminopeptidase (type 2) is the common target for angiogenesis inhibitors AGM-1470 and ovalicin, *Chem. Biol. 4*, 461−471.
12. Sin, N., Meng, L., Wang, M. Q., Wen, J. J., Bornmann, W. G., and Crews, C. M. (1997) The anti-angiogenic agent fumagillin covalently binds and inhibits the methionine aminopeptidase, MetAP-2, *Proc. Natl. Acad. Sci. U.S.A. 94*, 6099−6103.
13. Zhang, Y., Griffith, E. C., Sage, J., Jacks, T., and Liu, J. O. (2000) Cell cycle inhibition by the anti-angiogenic agent TNP-470 is mediated by p53 and p21WAF1/CIP1, *Proc. Natl. Acad. Sci. U.S.A. 97*, 6427−6432.
14. Yeh, J. R., Mohan, R., and Crews, C. M. (2000) The antiangiogenic agent TNP-470 requires p53 and p21CIP/WAF for endothelial cell growth arrest, *Proc. Natl. Acad. Sci. U.S.A. 97*, 12782−12787.
15. Hu, X., Addlagatta, A., Lu, J., Matthews, B. W., and Liu, J. O. (2006) Elucidation of the function of type 1 human methionine aminopeptidase during cell cycle progression, *Proc. Natl. Acad. Sci. U.S.A. 103*, 18148−18153.
16. Serero, A., Giglione, C., Sardini, A., Martinez-Sanz, J., and Meinnel, T. (2003) An unusual peptide deformylase features in the human mitochondrial N-terminal methionine excision pathway, *J. Biol. Chem. 278*, 52953−52963.
17. Leszczyniecka, M., Bhatia, U., Cueto, M., Nirmala, N. R., Towbin, H., Vattay, A., Wang, B., Zabludoff, S., and Phillips, P. E. (2006) MAP1D, a novel methionine aminopeptidase family member is overexpressed in colon cancer, *Oncogene 25*, 3471−3478.
18. Roderick, S. L., and Matthews, B. W. (1993) Structure of the cobalt-dependent methionine aminopeptidase from *Escherichia coli*: a new type of proteolytic enzyme, *Biochemistry 32*, 3907−3912.
19. Addlagatta, A., Quillin, M. L., Omotoso, O., Liu, J. O., and Matthews, B. W. (2005) Identification of an SH3-binding motif in a new class of methionine aminopeptidases from *Mycobacterium tuberculosis* suggests a mode of interaction with the ribosome, *Biochemistry 44*, 7166−7174.
20. Oefner, C., Douangamath, A., D'Arcy, A., Hafeli, S., Mareque, D., Mac, S. A., Padilla, J., Pierau, S., Schulz, H., Thormann, M., Wadman, S., and Dale, G. E. (2003) The 1.15A crystal structure of the *Staphylococcus aureus* methionyl-aminopeptidase and complexes with triazole based inhibitors, *J Mol. Biol. 332*, 13−21.
21. Tahirov, T. H., Oki, H., Tsukihara, T., Ogasahara, K., Yutani, K., Ogata, K., Izu, Y., Tsunasawa, S., and Kato, I. (1998) Crystal structure of methionine aminopeptidase from hyperthermophile, *Pyrococcus furiosus*, *J. Mol. Biol. 284*, 101−124.
22. Addlagatta, A., Hu, X., Liu, J. O., and Matthews, B. W. (2005) Structural basis for the functional differences between type I and type II human methionine aminopeptidases, *Biochemistry 44*, 14741−14749.
23. Cosper, N. J., D'souza, V. M., Scott, R. A., and Holz, R. C. (2001) Structural evidence that the methionyl aminopeptidase from *Escherichia coli* is a mononuclear metalloprotease, *Biochemistry 40*, 13302−13309.
24. Ye, Q. Z., Xie, S. X., Ma, Z. Q., Huang, M., and Hanzlik, R. P. (2006) Structural basis of catalysis by monometalated methionine aminopeptidase, *Proc. Natl. Acad. Sci. U.S.A. 103*, 9470−9475.
25. Schiffmann, R., Heine, A., Klebe, G., and Klein, C. D. (2005) Metal ions as cofactors for the binding of inhibitors to methionine aminopeptidase: a critical view of the relevance of in vitro metalloenzyme assays, *Angew. Chem., Int. Ed. 44*, 3620−3623.
26. Bolton, E. C., Mildvan, A. S., and Boeke, J. D. (2002) Inhibition of reverse transcription in vivo by elevated manganese ion concentration, *Mol. Cell 9*, 879−889.
27. Han, H., Rifkind, J. M., and Mildvan, A. S. (1991) Role of divalent cations in the 3′,5′-exonuclease reaction of DNA polymerase I, *Biochemistry 30*, 11104−11108.

28. Conyers, G. B., Wu, G., Bessman, M. J., and Mildvan, A. S. (2000) Metal requirements of a diadenosine pyrophosphatase from *Bartonella bacilliformis*: magnetic resonance and kinetic studies of the role of Mn^{2+}, *Biochemistry 39*, 2347−2354.
29. Fersht, A. (1999) *Structure and mechanism in protein science: A guide to enzyme catalysis and protein folding*, 2nd ed., W. H. Freeman and Co., New York.
30. Hu, X., Mildvan, A., and Liu, J. O. (2007) Cooperative activation of human mitochondrial Methionine Aminopeptidase (hmMetAP) by Co^{2+}, Abstracts from the Experimental Biology Meeting, Washington, DC, April 28−May 2, 2007, *FASEB J. 21*, A272; Abstr. 510.4.
31. Lowther, W. T., McMillen, D. A., Orville, A. M., and Matthews, B. W. (1998) The anti-angiogenic agent fumagillin covalently modifies a conserved active-site histidine in the *Escherichia coli* methionine aminopeptidase, *Proc. Natl. Acad. Sci. U.S.A. 95*, 12153−12157.
32. Zhou, Y., Guo, X. C., Yi, T., Yoshimoto, T., and Pei, D. (2000) Two continuous spectrophotometric assays for methionine aminopeptidase, *Anal. Biochem. 280*, 159−165.
33. O'Keeffe, E. T., Hill, R. L., and Bell, J. E. (1980) Active site of bovine galactosyltransferase: kinetic and fluorescence studies, *Biochemistry 19*, 4954−4962.
34. Hawkins, J., and Boden, M. (2006) Detecting and sorting targeting peptides with neural networks and support vector machines, *J. Bioinf. Comput. Biol 4*, 1−18.
35. Chenna, R., Sugawara, H., Koike, T., Lopez, R., Gibson, T. J., Higgins, D. G., and Thompson, J. D. (2003) Multiple sequence alignment with the Clustal series of programs, *Nucleic Acids Res. 31*, 3497−3500.
36. Tatusova, T. A., and Madden, T. L. (1999) BLAST 2 Sequences, a new tool for comparing protein and nucleotide sequences, *FEMS Microbiol. Lett. 174*, 247−250.
37. Andrade, M. A., Chacón, P., Merelo, J. J., and Morán, F. (1993) Evaluation of secondary structure of proteins from UV circular dichroism using an unsupervised learning neural network, *Protein Eng. 6*, 383−390.
38. Merelo, J. J., Andrade, M. A., Prieto, A., and Morán, F. (1994) Proteinotopic Feature Maps, *Neurocomputing 6*, 443−454.
39. Olesik, J. W. (1991) Elemental analysis using ICP-OES and ICP/MS, *Anal. Chem. 63*, 12A−21A.
40. Wang, J., Sheppard, G. S., Lou, P., Kawai, M., Park, C., Egan, D. A., Schneider, A., Bouska, J., Lesniewski, R., and Henkin, J. (2003) Physiologically relevant metal cofactor for methionine aminopeptidase-2 is manganese, *Biochemistry 42*, 5035−5042.
41. Schiffmann, R., Neugebauer, A., and Klein, C. D. (2006) Metal-mediated inhibition of *Escherichia coli* methionine aminopeptidase: structure-activity relationships and development of a novel scoring function for metal-ligand interactions, *J. Med. Chem. 49*, 511−522.
42. Hu, X., Addlagatta, A., Matthews, B. W., and Liu, J. O. (2006) Identification of Pyridinylpyrimidines as Inhibitors of Human Methionine Aminopeptidases, *Angew. Chem., Int. Ed. 45*, 3772−3775.
43. D'souza, V. M., and Holz, R. C. (1999) The methionyl aminopeptidase from *Escherichia coli* can function as an iron(II) enzyme, *Biochemistry 38*, 11079−11085.
44. Li, J. Y., Chen, L. L., Cui, Y. M., Luo, Q. L., Gu, M., Nan, F. J., and Ye, Q. Z. (2004) Characterization of full length and truncated type I human methionine aminopeptidases expressed from *Escherichia coli*, *Biochemistry 43*, 7892−7898.
45. Copik, A. J., Swierczek, S. I., Lowther, W. T., D'souza, V. M., Matthews, B. W., and Holz, R. C. (2003) Kinetic and spectroscopic characterization of the H178A methionyl aminopeptidase from *Escherichia coli*, *Biochemistry 42*, 6283−6292.
46. Gordon, D. M., Dancis, A., and Pain, D. (2000) Mechanisms of mitochondrial protein import, *Essays Biochem. 36*, 61−73.
47. Ben-Bassat, A., Bauer, K., Chang, S. Y., Myambo, K., Boosman, A., and Chang, S. (1987) Processing of the initiation methionine from proteins: properties of the *Escherichia coli* methionine aminopeptidase and its gene structure, *J. Bacteriol. 169*, 751−757.
48. D'souza, V. M., Bennett, B., Copik, A. J., and Holz, R. C. (2000) Divalent metal binding properties of the methionyl aminopeptidase from *Escherichia coli*, *Biochemistry 39*, 3817−3826.
49. Meinnel, T., Mechulam, Y., and Blanquet, S. (1993) Methionine as translation start signal: a review of the enzymes of the pathway in *Escherichia coli*, *Biochimie 75*, 1061−1075.
50. Bradshaw, R. A., and Yi, E. (2002) Methionine aminopeptidases and angiogenesis, *Essays Biochem. 38*, 65−78.
51. Chen, X. J., and Butow, R. A. (2005) The organization and inheritance of the mitochondrial genome, *Nat Rev. Genet. 6*, 815−825.
52. Berg, J. M., Tymoczko, J. L., and Stryer, L. (2002) Regulatory strategies: enzymes and hemoglobin, in *Biochemistry*, 5th ed., pp 280−283, W. H. Freeman, New York.
53. Mildvan, A. S. (1997) Mechanisms of signaling and related enzymes, *Proteins: Struct., Funct., Genet. 29*, 401−416.
54. Larrabee, J. A., Leung, C. H., Moore, R. L., Thamrong-nawasawat, T., and Wessler, B. S. (2004) Magnetic circular dichroism and cobalt(II) binding equilibrium studies of *Escherichia coli* methionyl aminopeptidase, *J Am. Chem Soc. 126*, 12316−12324.
55. Addlagatta, A., and Matthews, B. W. (2006) Structure of the angiogenesis inhibitor ovalicin bound to its noncognate target, human Type 1 methionine aminopeptidase, *Protein Sci. 15*, 1842−1848.
56. Lowther, W. T., Orville, A. M., Madden, D. T., Lim, S., Rich, D. H., and Matthews, B. W. (1999) *Escherichia coli* methionine aminopeptidase: implications of crystallographic analyses of the native, mutant, and inhibited enzymes for the mechanism of catalysis, *Biochemistry 38*, 7678−7688.
57. Huang, M., Xie, S. X., Ma, Z. Q., Hanzlik, R. P., and Ye, Q. Z. (2006) Metal mediated inhibition of methionine aminopeptidase by quinolinyl sulfonamides, *Biochem. Biophys. Res. Commun. 339*, 506−513.
58. Turk, B. E., Griffith, E. C., Wolf, S., Biemann, K., Chang, Y. H., and Liu, J. O. (1999) Selective inhibition of amino-terminal methionine processing by TNP-470 and ovalicin in endothelial cells. *Chem. Biol. 6*, 823−833.

BI701127X